JPEDAV (2005) 26:39-49
DOI: 10.1361/15477030522464
1547-7037/$19.00 ©ASM International

Thermodynamic Assessments of the Phase Diagrams of the Hafnium-Vanadium and Vanadium-Zirconium Systems

C. Servant

(Submitted May 17, 2004; in revised form November 9, 2004)

Thermodynamic assessments have been made for the hafnium-vanadium (Hf-V) and vanadium-zirconium (V-Zr) systems using the Calphad-Thermocalc approach. The Gibbs energies of the liquid, body-centered cubic, and close-packed hexagonal phases were described by a substitution solution model with a Redlich-Kister formalism to express the excess Gibbs energy. The *C*15-Laves phase was treated first as stoichiometric and then with a composition range. A consistent set of optimized thermodynamic parameters was obtained, and calculated phase equilibria were compared with the experimental data. The enthalpy of formation of the C15-Laves phase was calculated equal to approximately −3 and −5 kJ/mol, respectively, in the Hf-V and V-Zr systems, which is in good agreement with predicted values.

1. Introduction

The unmixing of transition metal carbide phases following the equation $(M_1,M_2)C \rightarrow M_1C + M_2C$ (M_i = Hf, Nb, Ta, Ti, V, Zr) has been experimentally observed in pseudobinary solid solution systems (Ref 1, 2) and also in more complex Fe-based systems (Ref 3). Furthermore, the possibility of such an unmixing has been frequently mentioned (Ref 4, 5) in steel systems to explain the striking differences in chemical composition of precipitated carbide or nitride phases, when more than one carbide former is present in the steel as an alloying element.

To describe phase separation in a pseudobinary solid solution system of the form $(M_1,M_2)C$, where M_1 and M_2 are chosen from among various elements (Hf, Nb, Ta, Ti, V, and Zr), it is necessary to assess the $(M_1$-$M_2)$ binary systems. In a previous article (Ref 6), the authors gave a thermodynamic evaluation of the tantalum-vanadium (Ta-V) system. Other already evaluated systems that can play a role in the description of complex refractory carbides include the hafnium-tantalum (Hf-Ta) (Ref 7), zirconium-niobium (Zr-Nb) (Ref 8), and zirconium-tantalum (Zr-Ta) (Ref 9) systems. In addition, a previous thermodynamic assessment of the vanadium-zirconium (V-Zr) system has been made by Korb and Hack (Ref 10), considering the C15-Laves phase as stoichiometric and the G(LiqV) and G(LiqZr) reference states for the thermodynamic functions of that phase.

The aim of the present work was to use the Calphad approach (Ref 11) for the assessment of the Hf-V binary system and the reassessment of the Hf-V system. In addition to their potential use in the study of carbide systems, the Hf-V and V-Zr systems are well known for forming Laves phases. The study of these Laves phases has evoked broad attention in fields such as hydrogen storage materials (Ref 12), superconducting behavior (Ref 13), and mechanical properties at room temperature (Ref 14), which provided further motivation for such an assessment. For both systems, the *C*15-Laves phase has been considered first as stoichiometric and then with a composition range. Furthermore, different references states were compared to account for the crystallographic structure of the *C*15-Laves phase and to obtain optimized thermodynamic parameters that keep coherency with the TCFe2000 database.

2. Thermodynamic Models and Available Thermodynamic Information

The systems Hf-V and V-Zr had to be optimized using mainly phase diagram data. Most of the information was taken from the File binary edition (Ref 15).

- In the case of the Hf-V system, the phase diagrams experimentally assessed in Ref 16 and 17 by means of x-ray, melting point, and differential thermal analysis, and metallographic techniques are very similar. The *C*15-Laves phase melts congruently at a temperature of 1552 °C (Ref 16) and 1550 °C (Ref 17), and has a homogeneity range. On the other hand, according to Komjathy (Ref 18), its melting point is higher (2173 °C) and the phase is stoichiometric. In the experimental work of Komjathy (Ref 18) concerning the extent of the V-rich solid solution between 800 and 1500 °C, the invariant reaction between HfV_2 and the solid solution, as well as the melt reactions were determined. Conflicting information is provided in Ref 19 and 20, studies in which the Laves phase formation was reported to occur as result of a peritectic reaction at either 1546 °C (Ref 19) or 1490 °C (Ref 20).

C. Servant, Laboratoire de Physico-Chimie de l'Etat Solide, UMR 8648, Université de Paris-Sud, 91405 Orsay Cedex, France. Contact e-mail: colette.servant@lpces.u-psud.fr.

Table 1 Thermodynamic data predicted by de Boer et al. (Ref 25) by using the method of Miedema et al. (Ref 26) and optimized data in the present work

	$\Delta H_{melting}$ 0.5 M_1-0.5 M_2 liquid phase (kJ/mol) at 25°C (298.15 K)		$\Delta H_{formation}$H Laves phase (kJ/mol) at 25°C (298.15 K)	
System M_1-M_2	**Ref 25, 26**	**Optimized data (present work)**	**Ref 25, 26**	**Optimized data (present work)**
Hf-V	−2	bcc_*A*2 V and cph_*A*3 Hf −5.528/−4.420 fcc_*A*1 V and bcc_*A*2 Hf −4.670/−4.692	−3	bcc_*A*2 V and cph_*A*3 Hf −3.344/−3.500 fcc_*A*1 V and bcc_*A*2 Hf −3.204/−2.813
V-Zr	−4	bcc_*A*2 V and cph_*A*3 Zr −4.350/−4.350 fcc_*A*1 V and bcc_*A*2 Zr −4.204/−3.920	−5	bcc_*A*2 V and cph_*A*3 Zr −5.000/−4.786 fcc_*A*1 V and bcc_*A*2 Zr −4.681/−5.181

The C15-Laves phase is considered as stoichiometric and with a composition range

- In the case of the V-Zr system, the experimental phase diagrams assessed by Smith (Ref 21) and Williams (Ref 22) are very similar. This system contains only one intermediate-phase V_2Zr that forms peritectically at 1300 °C. Vanadium takes a maximum of about 5 at.% Zr into solid solution, while βZr dissolves about 15 at.% V. The solubility of V in αZr is very low. The phase diagrams determined by Smith (Ref 21) and Williams (Ref 22) are in turn markedly different from those reported by Rostoker and Yamamoto (Ref 23) and Petrova (Ref 24), wherein V_2Zr forms at about 1740 °C. In this latter case, only the Zr-rich side of the phase diagram was determined. Only Smith (Ref 21) pointed out a composition range for the *C*15-Laves phase.

Furthermore, there is a considerable lack of thermodynamic data on these systems. In both cases, only the enthalpies of mixing of the liquid phase for the $0.5M_1$-$0.5M_2$ composition predicted at 25 °C (298.15 K) by de Boer et al. (Ref 25), using the method of Miedema et al. (Ref 26), as well as the enthalpy of formation of the *C*15-Laves phases are available in the literature. They are listed in Table 1.

From the crystallographic point of view, the Laves phase (determined in both systems as *C*15, prototype $MgCu_2$, Pearson symbol *cF*24 (Ref 27)) contains two distinct Wyckoff positions, namely, 8(a) (coordination number 16) and 16(d) (coordination number 12). A two-sublattice model is thus a reasonable choice for the thermodynamic description of this phase. As the experimentally determined homogeneity range is small, if it exists, and its limits are not quite sure, the authors adopted its extension on both sides of the stoichiometric composition, that is, the formula $(M_1,M_2)_{0.66667}(M_1,M_2)_{0.33333}$. The authors' approach is a preliminary one because they have no experimental information on the nature of the defects (substitution or vacancies) that account for the nonstoichiometric width when it is indicated.

The accepted criterion used to define the reference state for the thermodynamic functions of the *C*15-Laves phase is to assign the face-centered cubic (fcc)_*A*1 reference state to species occupying a site with coordination 12, and the body-centered cubic (bcc)_*A*2 reference state for species occupying a site with coordination > 12. For instance, in the current status of the TCFe2000 database that is true for the systems iron-niobium and iron-tungsten. However, to keep coherence with the existing description of the Laves phases in other systems such as Cr-Ta (Ref 28) and Cr-Ni-Ta (Ref 29), the authors have also made assessments by defining the reference state as bcc_*A*2 V and hexagonally close-packed (cph)_*A*3 Hf (or cph_*A*3 Zr), irrespective of coordination number. This was done because all of these Laves phases could play a role in broader thermodynamic databases related to steels.

The substitutional solution phases for the optimized binary systems were modeled:

- One sublattice for the liquid phase: $(M_1,M_2)_1$
- Two sublattices for the bcc_A2 phase: $(M_1,M_2)_1$: $(Va)_3$
- Two sublattices for the fcc_A1 phase: $(M_1,M_2)_1$: $(Va)_1$
- Two sublattices for the cph_A3 phase: $(M_1,M_2)_1$: $(Va)_{0.5}$

The *C*15-Laves phases, HfV_2 and V_2Zr, of the binary systems Hf-V and V-Zr were first modeled as stoichiometric $(M1)_{0.33333}$ $(M2)_{0.66667}$, and then with a two-sublattice description with a mutual substitution in each sublattice $(M_1,M_2)_{0.33333}$ $(M_1,M_2)_{0.66667}$, as mentioned above. The sublattice formalism used here is identical to that of the Wagner-Schottky model (Ref 30).

The complete description of this phase is:

$$\begin{aligned} {}^{\mathrm{ref}}G^{C15\text{-Laves}} &= y'_{\mathrm{M1}}y''_{\mathrm{M2}}\,{}^{0}G^{C15\text{-Laves}}_{\mathrm{M1:M2}} + y'_{\mathrm{M1}}y''_{\mathrm{M1}}\,{}^{0}G^{C15\text{-Laves}}_{\mathrm{M1:M1}} \\ &\quad + y'_{\mathrm{M2}}y''_{\mathrm{M2}}\,{}^{0}G^{C15\text{-Laves}}_{\mathrm{M2:M2}} + y'_{\mathrm{M2}}y''_{\mathrm{M1}}\,{}^{0}G^{C15\text{-Laves}}_{\mathrm{M2:M1}} \end{aligned} \qquad \text{(Eq 1)}$$

$$\begin{aligned} {}^{0}G^{C15\text{-Laves}}_{\mathrm{M1:M2}} &= 0.33333 \times {}^{0}G^{\mathrm{bcc\_}A2}_{\mathrm{M1}} \\ &\quad + 0.66667 \times {}^{0}G^{\mathrm{fcc\_}A1}_{\mathrm{M2}} + a + bT \end{aligned} \qquad \text{(Eq 2)}$$

$$\begin{aligned} {}^{\mathrm{id}}G^{C15\text{-Laves}} &= RT[0.33333 \times (y'_{\mathrm{M1}}Lny'_{\mathrm{M1}} + y'_{\mathrm{M2}}Lny'_{\mathrm{M2}}) \\ &\quad + 0.66667 \times (y''_{\mathrm{M1}}Lny''_{\mathrm{M1}} + y''_{\mathrm{M2}}Lny''_{\mathrm{M2}})] \end{aligned} \qquad \text{(Eq 3)}$$

$$\begin{aligned} {}^{\mathrm{E}}G^{C15\text{-Laves}} &= y'_{\mathrm{M1}}y'_{\mathrm{M2}}(y''_{\mathrm{M1}}\,{}^{0}L^{C15\text{-Laves}}_{\mathrm{M1,M2:M1}} + y''_{\mathrm{M2}}\,{}^{0}L^{C15\text{-Laves}}_{\mathrm{M1,M2:M2}}) \\ &\quad + y''_{\mathrm{M1}}y''_{\mathrm{M2}}(y'_{\mathrm{M1}}\,{}^{0}L^{C15\text{-Laves}}_{\mathrm{M1:M1,M2}} + y'_{\mathrm{M2}}\,{}^{0}L^{C15\text{-Laves}}_{\mathrm{M2:M1,M2}}) \\ &\quad + y'_{\mathrm{M1}}y'_{\mathrm{M2}}y''_{\mathrm{M1}}y''_{\mathrm{M2}}\,{}^{0}L^{C15\text{-Laves}}_{\mathrm{M1,M2:M1,M2}} \end{aligned} \qquad \text{(Eq 4)}$$

$${}^{0}G^{C15\text{-Laves}}_{\mathrm{M1:M2}} = -{}^{0}G^{C15\text{-Laves}}_{\mathrm{M2:M1}} + {}^{0}G^{C15\text{-Laves}}_{\mathrm{M1:M1}} + {}^{0}G^{C15\text{-Laves}}_{\mathrm{M2:M2}} \qquad \text{(Eq 5)}$$

where y'_i and y''_i refer to the sites fractions of the component *i* in the first and second sublattices, respectively. In Eq 2, *a* and *b* are coefficients to be optimized. The four terms denoted $^{0}G^{C15\text{-Laves}}$ represent the Gibbs energies of the stable and metastable stoichiometric compounds $M1M1_2$, $M1M2_2$, $M2M1_2$, and $M2M2_2$. The excess parameters $^{0}L^{C15\text{-Laves}}$ in Eq 4 account for the interaction of species in each sublattice. Finally, Eq 5 accounts for the Wagner-Schottky constraint (Ref 30).

The molar Gibbs energies of formation of the hypothetical phase formed with pure elements were fixed at a value

Table 2 Comparison of the experimental and calculated data for the Hf-V binary system assuming a stoichiometric *C*15-Laves phase

	Calculated *T* (°C) *x*Hf (at.%) (this work)(a)		Experimental *T* (°C) and *x*Hf (at.%)
Invariant equilibria(b)	**cph_*A*3 Hf and bcc_*A*2 V**	**bcc_*A*2 Hf and fcc_*A*1 V**	
Congruent melting	1529	1534	1552 (Ref 16) 0.341
L ↔ *C*15-Laves	0.333	0.333	1550 (Ref 17) 0.335
Eutectic reaction	1528	1533	1520 (Ref 16, 17)
L → bcc_*A*2 + *C*15-Laves	0.316 → 0.025 + 0.333	0.313 → 0.033 + 0.333	0.309 → 0.041 + 0.331 (Ref 16)
			0.311 → 0.041 + 0.331 (Ref 17)
Eutectic reaction	1456	1459	1453 (Ref 16), 1456 (Ref 17)
Liq → bcc_*A*2 + *C*15-Laves	0.547 → 0.743 + 0.333	0.541 → 0.750 + 0.333	0.572 → 0.767 + 0.354 (Ref 16)
			0.570 → 0.765 + 0.355 (Ref 17)
Eutectoid reaction	1210	1204	1193 (Ref 16), 1190 (Ref 17)
bcc_*A*2 → *C*15-Laves + cph_*A*3	0.813 → 0.333 + 0.972	0.822 → 0.333 + 0.981	0.812 → 0.353 + 0.987 (Ref 16)
			0.810 → 0.351 + 0.978 (Ref 17)
Predicted (Ref 25)	−2000	−2000	…
Calculated (this work) HMR (liquid 0.5Hf-0.5V) (J/mol) at 25 °C (298.15 K) with the reference state liquid for Hf and V at 25 °C (298.15 K)	−5528	−4670	…
Predicted (Ref 25)	−3000	−3000	…
Calculated (this work) HMR (*C*15-Laves) (J/mol) at 25 °C (298.15 K)	−3344	−3204	…

(a) The reference states are first, the cph_*A*3 Hf and bcc_*A*2 V, then bcc_*A*2 Hf and fcc_*A*1 V. (b) HMR, enthalpy of mixing of the liquid phase or enthalpy of formation of the *C*15-Laves phase

Table 3 Comparison of the experimental and calculated data for the Hf-V binary system assuming a *C*15-Laves phase with a composition range

	Calculated *T* (°C) and *x*(Hf) (at.%) (this work)(a)		Experimental *T* (°C) and *x*(Hf) (at.%)
Invariant equilibria(b)	**cph_*A*3 Hf and bcc_*A*2 V**	**bcc_*A*2 Hf and fcc_*A*1 V**	
Congruent melting	1536	1532.5	1552 (Ref 16) 0.341
L ↔ *C*15 Laves	0.328	0.339	1550 (Ref 17) 0.335
Eutectic reaction	1535	1531	1520 (Ref 16, 17)
L → bcc_*A*2 + *C*15-Laves	0.308 → 0.027 + 0.325	0.309 → 0.033 + 0.336	0.309 → 0.041 + 0.331 (Ref 16)
			0.311 → 0.041 + 0.331 (Ref 17)
Eutectic reaction	1460	1458	1453 (Ref 16), 1456 (Ref 17)
L → bcc_*A*2 + *C*15-Laves	0.540 → 0.757 + 0.360	0.545 → 0.755 + 0.361	0.572 → 0.767 + 0.354 (Ref 16)
			0.570 → 0.765 + 0.355 (Ref 17)
Eutectoid reaction	1193	1200	1993 (Ref 16), 1190 (Ref 17)
bcc_*A*2 → *C*15-Laves + cph_*A*3	0.814 → 0.355 + 0.974	0.819 → 0.352 + 0.980	0.812 → 0.353 + 0.987 (Ref 16)
			0.810 → 0.351 + 0.978 (Ref 17)
Predicted (Ref 25)	−2000	−2000	…
Calculated (this work) HMR (liquid 0.5Hf-0.5V) (J/mol) at 25 °C (298.15 K) with the reference state liquid for Hf and V at 25 °C (298.15 K)	−4420	−4692	at 25 °C (298.15 K)
Predicted (Ref 25)	−3000	−3000	…
Calculated (this work) HMR (*C*15-Laves) (J/mol) at 25 °C (298.15 K)	−3500	−2813	…

(a) The reference states are first, the cph_*A*3 Hf and bcc_*A*2 V, then bcc_*A*2 Hf and fcc_*A*1 V. (b) HMR, enthalpy of mixing of the liquid phase or enthalpy of formation of the *C*15-Laves phase

5000 J/mol of atoms to be consistent with the thermodynamic description of systems in the TCFe2000 database.

The Gibbs energy per mole of atoms of the liquid, bcc_*A*2, and cph_*A*3 substitutional solution phases at 101,325 Pa was described using:

$$G_M^{\phi} = x_{M1}\,{}^0G_{M1}^{\phi} + x_{M2}\,{}^0G_{M2}^{\phi} + RT(x_{M1}\ln x_{M1} + x_{M2}\ln x_{M2}) + {}^EG_M^{\phi} \qquad \text{(Eq 6)}$$

where x_i (i = M_1,M_2) represents the atomic fraction of the element I, and ${}^0G_i^{\phi}$ (with ϕ = liquid, bcc_*A*2, and cph_*A*3) is the molar Gibbs energy of the element i with the structure ϕ. The ${}^0G_i^{\phi}$ values are referred to the enthalpy H of the standard reference state (SER) of the pure solid elements in their stable form (cph_*A*3 Hf (or Zr) and bcc_*A*2 V) at 25 °C (298.15 K), as proposed by the Scientific Group Thermodata Europe. The ${}^0G_i^{\phi}$-H_{Mi}^{SER} data published by Dinsdale (Ref 31) were used for the thermodynamic functions of the pure elements. The excess Gibbs energy ${}^EG_M^{\phi}$ was described by means of a Redlich-Kister polynomial (Ref 32):

$${}^EG_M^{\phi} = x_{M1}x_{M2}\left[{}^0L^{\phi} + {}^1L^{\phi}(x_{M1} - x_{M2})^1 + {}^2L^{\phi}(x_{M1} - x_{M2})^2\right] \qquad \text{(Eq 7)}$$

According to the experimental data available for each system, the liquid and bcc_*A*2 phases were treated in the regular, subregular, or subsubregular solution approximation (Ref 33), while the cph_*A*3 phase was treated as a regular solid solution. The composition interaction parameters ${}^iL^{\phi}$ are temperature-dependent:

$${}^iL^{\phi} = a + bT \qquad \text{(Eq 8)}$$

Due to a lack of experimental information in both systems, as few thermodynamic parameters as possible were chosen to model the different phases. These parameters were optimized using the Parrot module implemented in the Thermocalc software (Ref 34).

For both binary systems, the optimization was conducted as follows: first the *C*15-Laves phase was considered as stoichiometric, then the Laves phase was modeled with a mutual substitution of each element in the two sublattices to account for the narrow composition range displayed in the phase diagram.

3. Results and Discussion

3.1 Hf-V Binary System

The optimization was made by using the phase diagram data from Ref 16 and 17, which were very similar, while the data from Ref 18 to 20 were discarded. The enthalpy of the mixing of the equiatomic liquid phase and the enthalpy of formation of the *C*15-Laves phase, predicted by Ref 25 at 25.15 °C (298.15 K), were the only thermodynamic data available in the literature. In a first step, these two later sets of data were used for the optimization. The curve of the calculated enthalpy of mixing of the liquid phase versus the mole fraction of Hf was not monotonous and showed a maximum of small amplitude on the V-rich side. As the thermodynamic data evaluated by means of the method of Miedema et al. (Ref 26) should be utilized with caution, and as there are no experimental data in this region, in a second step, the enthalpy of mixing of the equiatomic liquid phase was discarded and a reasonable shape was obtained for that curve.

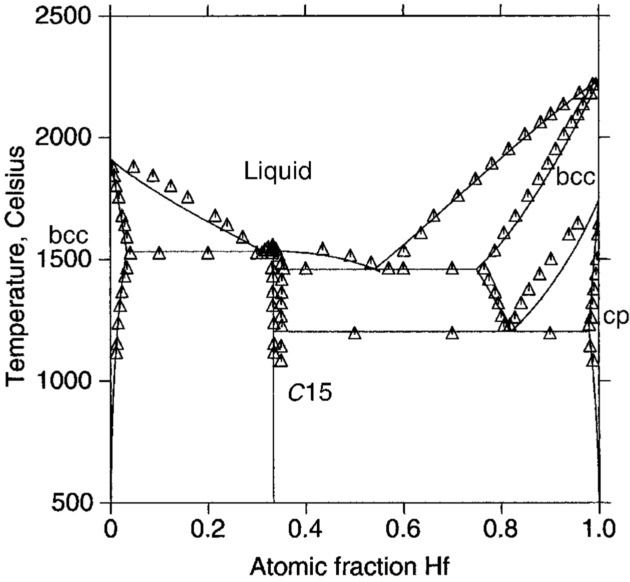

Fig. 1 Comparison of the experimental (Ref 16, 17) and calculated Hf-V phase diagrams with the *C*15-Laves phase being considered as stoichiometric; the reference states are bcc_*A*2 Hf and fcc_*A*1 V

The optimized parameters are reported in Appendix 1.

The results of the calculations based on the Calphad approach along with those reported in Ref 16 and 17 are summarized in Table 2 for the stoichiometric modeling of the *C*15-Laves phase. Table 3 contains the results obtained when the *C*15-Laves phase presents a composition range. The reference states assumed are first bcc_*A*2 V and cph_*A*3 Hf, and then bcc_*A*2 Hf and fcc_*A*1 V.

The measured and calculated phase diagrams are shown in Fig. 1 for the case of the stoichiometric *C*15 phase with the reference states bcc_*A*2 Hf and fcc_*A*1 V. A good agreement is obtained. The congruent melting temperature of the *C*15-Laves phase is 1534 °C.

In Fig. 2(a), the Hf-V calculated phase diagram (obtained by considering the *C*15-Laves phase with a composition range and with the reference states bcc_*A*2 Hf and fcc_*A*1 V) is compared with the experimental one. An enlargement of the congruent point is shown in Fig. 2(b).

Figure 3 shows the calculated enthalpy of mixing of the liquid phase in the Hf-V binary system (solid line). A reasonable shape is obtained. The calculated enthalpy of mixing of the equiatomic liquid (−4670 J/mol) is more negative than the only prediction (−2000 J/mol) by de Boer et al. (Ref 25) using the method of Miedema et al. (Ref 26).

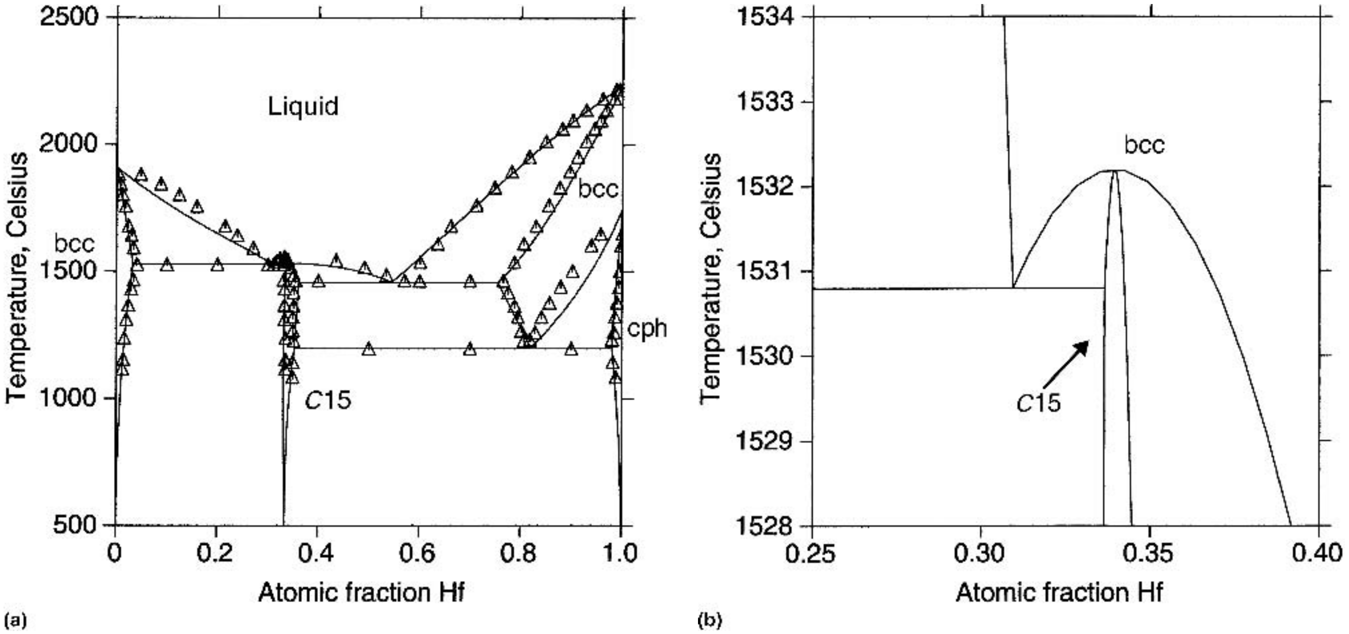

Fig. 2 (a) Comparison of the experimental (Ref 16, 17) and calculated Hf-V phase diagrams with the *C*15-Laves phase being considered with a composition range, with the reference states bcc_*A*2 Hf and fcc_*A*1 V). (b) Enlarged region near the congruent melting of the HfV_2 *C*15-Laves phase

Table 4 Comparison of the experimental (Ref 21, 22) and calculated data for the V-Zr binary system assuming a stoichiometric *C*15-Laves phase

	Calculated *T* (°C) and *x*(Zr) (at.%) (this work)(a)		
Invariant equilibria(b)	**cph_*A*3 Zr and bcc_*A*2 V**	**bcc_*A*2 Zr and fcc_*A*1 V**	**Experimental *T* (°C) and *x*(Zr) (at.%)**
Peritectic reaction	1299	1324	1300 (Ref 21, 22)
L + bcc_*A*2 → *C*15-Laves	0.490 + 0.061 → 0.333	0.462 + 0.053 → 0.333	0.478 + 0.048 → 0.333 (Ref 21)
			0.476 + 0.065 → 0.333 (Ref 22)/1279.7 (Ref 10)
			0.494 + 0.046 → 0.333 (Ref 10)
Eutectic reaction	1256	1255	1265 (Ref 21), 1227 (Ref 22)
L → *C*15-Laves + bcc_*A*2	0.550 → 0.333 + 0.820	0.564 → 0.333 + 0.830	0.571 → 0.350 + 0.825 (Ref 21)
			0.560 → 0.333 + 0.835 (Ref 22)
			1237.2 (Ref 10)
			0.548 → 0.333 + 0.839 (Ref 10)
Eutectoid reaction	770	770	777 (Ref 21), 780 (Ref 22)
bcc_*A*2 → *C*15-Laves + cph_*A*3	0.906 → 0.333 + 0.946	0.919 → 0.333 + 0.961	0.914 → 0.344 + 0.987 (Ref 21)
			0.900 → 0.333 + 1.000 (Ref 22)
			789.9 (Ref 10)
			0.927 → 0.333 + 0.959 (Ref 10)
Predicted (Ref 25)	−4000	−4000	…
Calculated (this work) HMR (liquid 0.5V-0.5Zr) (J/mol) at 25 °C (298.15 K) with the reference state liquid for Zr and V at 25 °C (298.15 K)	−4350	−4204	…
Predicted (Ref 25)	−5000	−5000	…
Calculated (this work) HMR (*C*15-Laves) (J/mol) at 25 °C (298.15 K)	−5000	−4681	…

(a) The reference states are first, the cph_*A*3 Zr and bcc_*A*2 V, then bcc_*A*2 Zr and fcc_*A*1 V. (b) HMR, enthalpy of mixing of the liquid phase or enthalpy of formation of the *C*15-Laves phase

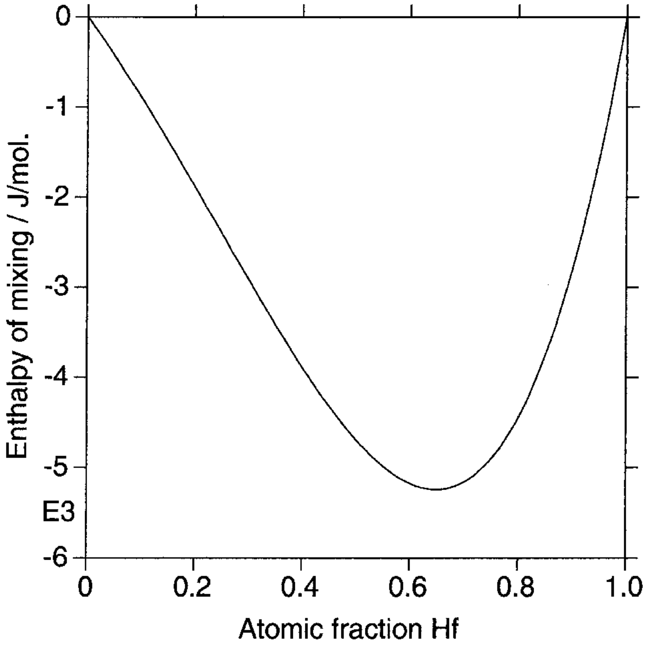

Fig. 3 Calculated enthalpies of mixing of the liquid phase in the Hf-V system (solid line)

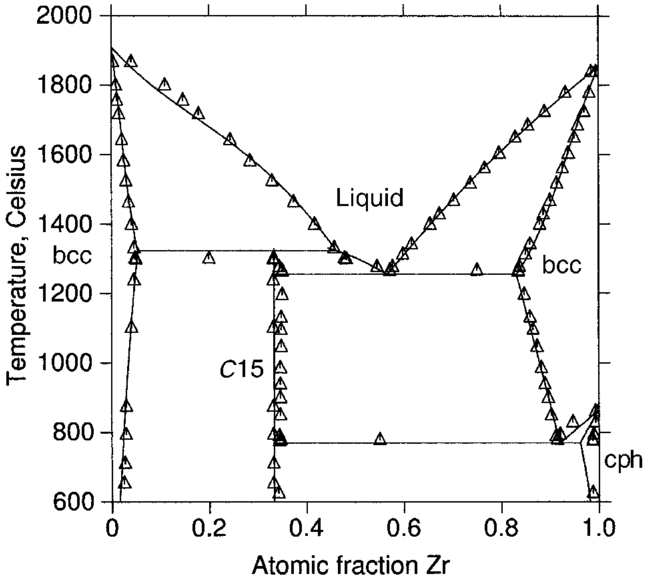

Fig. 4 Comparison of the experimental (Ref 21, 22) and calculated V-Zr phase diagrams with the *C*15-Laves phase being considered as stoichiometric; the reference states are bcc_*A*2 Zr and fcc_*A*1 V

Table 5 Comparison of the experimental and calculated data for the V-Zr binary system assuming a *C*15-Laves phase with a composition range

	Calculated *T* (°C) and *x*(Zr) (at.%) (this work)(a)		Experimental *T* (°C) and *x*(Zr) (at.%)
Invariant equilibria(b)	cph_*A*3 Zr and bcc_*A*2 V	bcc_*A*2 Zr and fcc_*A*1 V	
Peritectic reaction	1313	1319	1300 (Ref 21, 22)
L + bcc_*A*2 → *C*15-Laves	0.478 + 0.049 → 0.335	0.464 + 0.053 → 0.342	0.478 + 0.048 → 0.333 (Ref 21)
			0.476 + 0.065 → 0.333 (Ref 21)
Eutectic reaction	1252	1253	1265 (Ref 21), 1227 (Ref 22)
L → *C*15-Laves + bcc_*A*2	0.561 → 0.352 + 0.831	0.565 → 0.352 + 0.830	0.571 → 0.350 + 0.835 (Ref 21)
			0.560 → 0.333 + 0.835 (Ref 22)
Eutectoid reaction	773	771	771 (Ref 21), 780 (Ref 22)
bcc_*A*2 → *C*15-Laves + cph_*A*3	0.922 → 0.343 + 0.969	0.923 → 0.338 + 0.967	0.914 → 0.344 + 0.987 (Ref 21)
			0.900 → 0.333 + 1.000 (Ref 22)
Predicted (Ref 25)	−4000	−4000	…
Calculated (this work) HMR (liquid 0.5V-0.5Zr) (J/mol) at 25 °C (298.15 K) with the reference state liquid for Zr and V at 25 °C (298.15 K)	−4350	−3920	…
Predicted (Ref 25)	−5000	−5000	…
Calculated (this work) HMR (*C*15-Laves) (J/mol) at 25 °C (298.15 K)	−4786	−5181	…

(a) The reference states are first, bcc_*A*2 Zr and fcc_*A*1 V, then bcc_*A*2 Zr and fcc_*A*1 V. (b) HMR, enthalpy of mixing of the liquid phase or enthalpy of formation of the *C*15-Laves phase

3.2 V-Zr Binary System

The optimization was made by using the phase diagram data of Ref 21 and 22, which are very similar, and those of Ref 23 were discarded, as well as those of Ref 24, which concerned only the Zr-enriched part of the V-Zr phase diagram. As in the case of the Hf-V system, the enthalpy of mixing of the equiatomic liquid phase and the enthalpy of formation of the *C*15-Laves phase, predicted by Ref 25 at 298.15 K, were the only thermodynamic data available in the literature. These two latter sets of data were used in the optimization.

The optimized parameters are reported in the Appendix.

The results of the calculations based on the Calphad approach, along with those reported in Ref 21 and 22, as well as in Ref 10, are summarized in Table 4 for the stoichiometric modeling of the *C*15-Laves phase, and in Table 5 when the *C*15-Laves phase presents a composition range. The assumed reference states are first cph_*A*3 Zr and bcc_*A*2 V, and then bcc_*A*2 Zr and fcc_*A*1 V.

The measured and calculated V-Zr phase diagrams are shown in Fig. 4 in the case of the stoichiometric *C*15 phase with the reference states bcc_*A*2 Zr and fcc_*A*1 V. A very good agreement is shown.

The measured and calculated V-Zr phase diagrams are shown in Fig. 5 in the case of the *C*15 phase with a composition range and with the reference states bcc_*A*2 Zr and fcc_*A*1 V. A very good agreement is shown.

The calculated enthalpy of mixing of the liquid phase in the V-Zr binary system (solid line) compared with the prediction of de Boer et al. (Ref 25) using the method of Miedema et al. (Ref 26) (symbol) is shown in Fig. 6.

Contrary to the results for the Hf-V system that are assessed in the present work, a good agreement is obtained, as previously mentioned, in the Hf-Ta (Ref 7), Zr-Nb (Ref 8), and Zr-Ta (Ref 9) systems.

The authors have calculated the enthalpies of formation of the solid phases bcc_*A*2 and cph_*A*3 in the Hf-V system at 25 °C (298.15 K), with the respective reference states bcc-*A*2 V and bcc_*A*2 Hf, and cph_*A*3 V and cph_*A*3 Hf. These two phases do not have similar enthalpies of formation, as previously mentioned in Ref 7 in the case of the Hf-Ta system. The cph_*A*3 phase was described with a regular solution approximation (one excess thermodynamic parameter of degree 0), and its composition dependence is symmetrical on both sides of $x(\mathrm{V}) = 0.5$. On the contrary, the bcc_*A*2 phase was described with a subsubregular approximation (three excess thermodynamic parameters of respective degrees 0, 1, and 2). This last phase displays a deviation from the symmetrical behavior. In Fig. 7(a), the calculated enthalpies of formation of the bcc_*A*2 and cph_*A*3 solid solutions are compared with the predictions of de Boer et al. (Ref 25) of the ordered compounds of the Hf-V system. Contrary to the results obtained in Ref 7 in the case of the Hf-Ta system, the enthalpies of formation of the ordered compounds of the Hf-V system are negative, and are far from the trends of the cph_*A*3 and bcc_*A*2 solid solutions, the enthalpies of formation of which are positive. The same result was obtained for the V-Zr system (Fig. 7b).

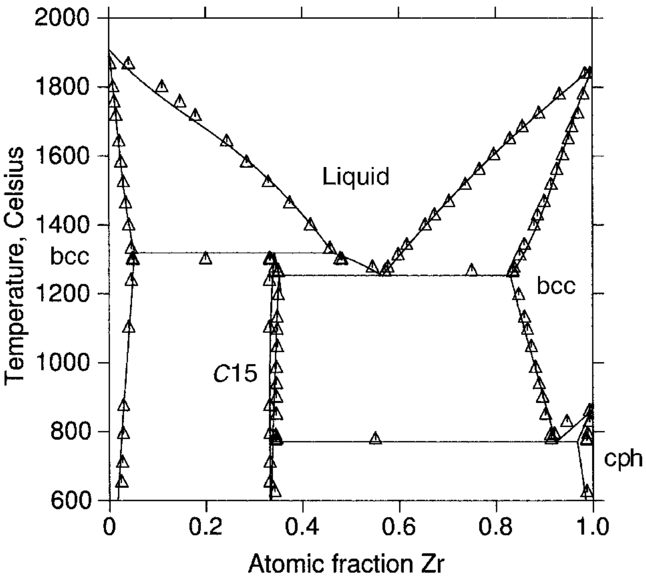

Fig. 5 Comparison of the experimental (Ref 21, 22) and calculated V-Zr phase diagrams with the *C*15-Laves phase being considered with a composition range; the reference states are bcc_*A*2 Zr and fcc_*A*1 V.

Despite the lack of thermodynamic data, the agreement between the experimental and calculated phase diagrams is satisfactory for both the Hf-V and V-Zr systems.

For these systems, the authors verified, following the objections of Zhang et al. (Ref 35) concerning the sublattice modeling, that the optimized thermodynamic parameters of the *C*15-Laves phase do not imply its formation at very high temperatures when the liquid phase is suspended during the calculation of the phase diagram. Instead, this phase transforms correctly into the disordered bcc_*A*2 phase, a fact that is illustrated in Fig. 8(a) and (b) in the case of the Hf-V system. This occurs when the *b* parameter of Eq 3 is positive (i.e., the entropy of formation is negative), so that the Gibbs energy of the *C*15-Laves phase decreases according to the formula $G = H - TS$ when the temperature increases.

4. Conclusion

The phase diagrams of the Hf-V and V-Zr binary systems have been assessed using the Calphad approach. Because very few thermodynamic data were available, the assessment was performed mainly on the basis of phase diagram data. The authors' results, however, are in good agreement with the predicted enthalpies of formation of the *C*15-Laves phase for both systems and with the predicted enthalpy of mixing of the equiatomic liquid phase only in the case of the V-Zr system. For both systems, the optimized thermodynamic parameters for the solution phases (i.e., liquid, bcc_*A*2 and cph_*A*3) are close, regardless of whether or not the *C*15-Laves phase was considered stoichiometric or to have a limited range of composition, or whether or not the crystal structure is formed with the elements (bcc_*A*2 V or fcc_*A*1 V) located on the sites of 12-fold coordination or (cph_*A*3 Hf (Zr) or bcc_*A*2 Hf (Zr)) located on the sites of a 16-fold coordination number. To calculate the unmixing of transition metal carbide phases (Ref 36), the presently optimized thermodynamic parameters for the Hf-V and V-Zr systems will be merged into a database for the C-Hf-V and C-V-Zr ternary systems with those being currently optimized from data determined on a physical basis in Ref 37.

Acknowledgment

The author acknowledges A. Danon, Centro Atomico Constituyentes, Comision Nacional de Energia Atomica, Av. Gral Paz 1499, 1650 San Martin Provincia de Buenos Aires, Argentina, for helpful discussions.

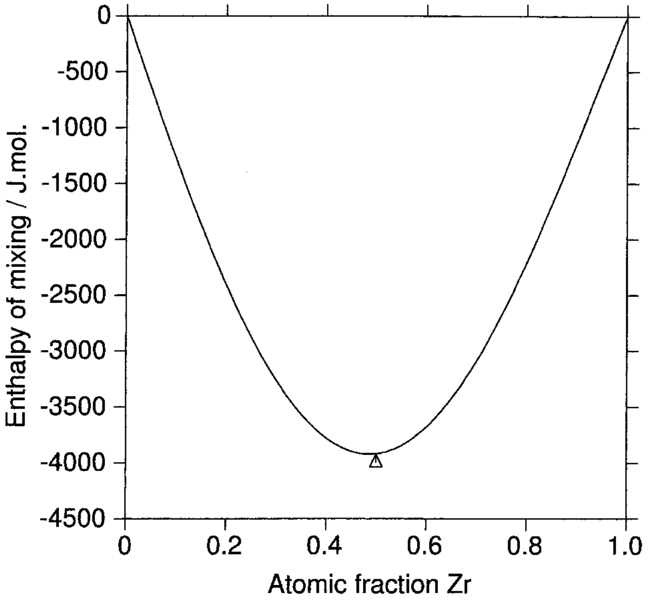

Fig. 6 Calculated enthalpies of mixing of the liquid phase in the V-Zr system (solid line). Comparison of the enthalpy of mixing of the equiatomic liquid phase with the one predicted by de Boer et al. (Ref 25) using the Miedema method (Ref 26) (symbols).

Appendix 1. Thermodynamic Properties of the Compounds and Solution Phases

The energies are given in Joules per mole, the temperature in degrees Kelvin.

The thermodynamic properties of the pure elements have been obtained from Dinsdale (Ref 31).

I. Hf-V System

I-1. C15-Laves Phase with Reference States cph_A3 Hf and bcc_A2 V

I-1-1. Modeling of the $C15$-Laves Phase as Stoichiometric: $\mathrm{Hf}_{0.33333}\mathrm{V}_{0.66667}$

$L(\text{liquid, Hf,V;0}) = -20{,}910.4353 + 13.3729{*}T$

$L(\text{liquid, Hf,V;1}) = -18{,}615.7038 + 4.1206{*}T$

$L(\text{liquid, Hf,V;2}) = -5168.9233$

$L(\text{bcc\_}A2\text{, Hf,V;0}) = 16{,}753.4911 + 7.6642{*}T$

$L(\text{bcc\_}A2\text{, Hf,V;1}) = -5012.0000 - 6.1986{*}T$

$L(\text{bcc\_}A2\text{, Hf,V;2}) = 3370.6775$

$L(\text{cph\_}A3\text{, Hf,V;0}) = 33{,}570.0000 + 0.1000{*}T$

$G(C15\text{-LAVES,Hf:V;0}) - 0.33333{*}H298(\text{CPH\_}A3\text{,Hf;0}) - 0.66667{*}\,H298(\text{BCC\_}A2\text{,V;0}) = -3600.0 + 0.1{*}T + 0.33333{*}\text{GHSERHF} + 0.66667{*}\text{GHSERVV}$

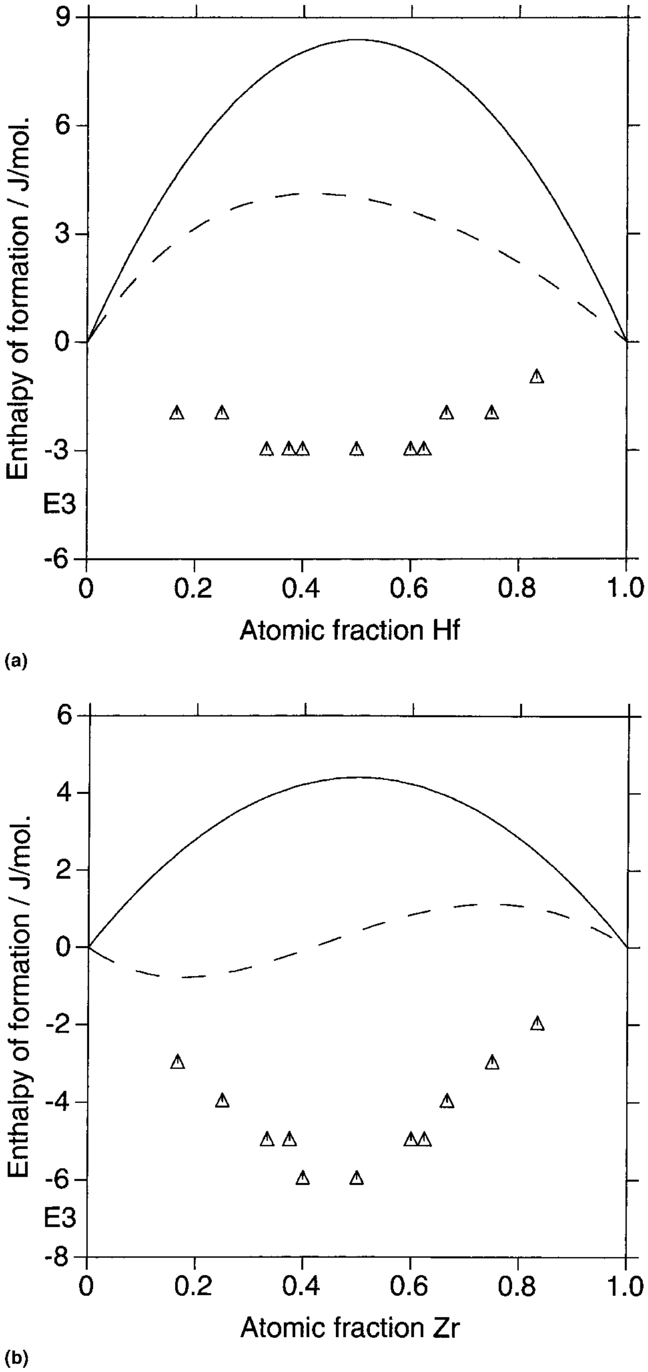

Fig. 7 Comparison of the enthalpies of formation of the bcc_$A2$ and cph_$A3$ solid solutions (respectively dashed and solid lines), calculated at 25 °C (298.15 K), with the predictions for the ordered compounds by de Boer et al. (Ref 25) (symbols) for the systems (a) Hf-V and (b) V-Zr

I-1-2. Modeling of the $C15$-Laves Phase with a Composition Range: $(\mathrm{Hf,V})_{0.33333}(\mathrm{Hf,V})_{0.66667}$

$L(\text{liquid, Hf,V;0}) = -17{,}678.0992 + 11.0841{*}T$

$L(\text{liquid, Hf,V;1}) = -10{,}157.4250 + 0.1428{*}T$

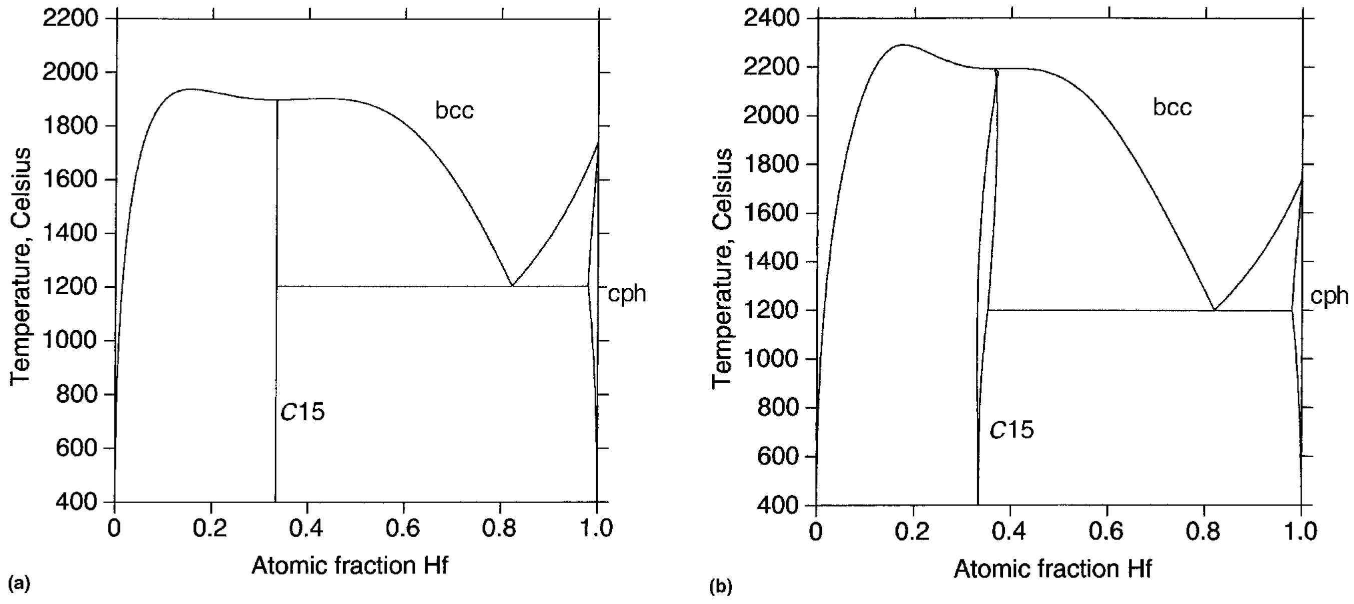

Fig. 8 Calculated phase diagram of the Hf-V system when the liquid phase is not considered and the C15-Laves phase is considered (a) as stoichiometric and (b) with a composition range; the reference states are bcc_A2 Hf and fcc_A1 V.

L(liquid, Hf,V;2) = −2957.9038

L(bcc_A2, Hf,V;0) = 13,364.8240 + 9.5488*T

L(bcc_A2, Hf,V;1) = −5012.0000 − 5.8727*T

L(bcc_A2, Hf,V;2) = 2311.9616

L(cph_A3, Hf,V;0) = 33,570.0000 + 0.1000*T

G(C15-LAVES,Hf:Hf;0) − H298(CPH_A3,Hf;0) = +5000 + GHSERHF

G(C15-LAVES,V:V;0) − H298(BCC_A2,V;0) = +5000 + GHSERVV

G(C15-LAVES,Hf:V;0) − 0.33333*H298(CPH_A3,Hf;0) − 0.66667* H298(BCC_A2,V;0) = − 3500 + 0.3699*T + 0.33333*GHSERHF + 0.66667*GHSERVV

G(C15-LAVES,V:Hf;0) − 0.33333*H298(BCC_A2,V;0) − 0.66667*H298(CPH_A3,Hf;0) = 3500 − 0.3699*T + 0.33333*GHSERVV + 0.66667*GHSERHF + 10,000

L(C15-LAVES,Hf:Hf,V;0) = 23,135.3046

L(C15-LAVES,V:Hf,V;0) = 9373.4171

I-2. C15-Laves Phase with Reference States bcc_A2 Hf and fcc_A1 V

I-2-1. Modeling of the C15-Laves Phase as Stoichiometric: $Hf_{0.33333}V_{0.66667}$

L(liquid, Hf,V;0) = −18,678.7073 + 11.3661*T

L(liquid, Hf,V;1) = −10,277.6548 + 0.1963*T

L(liquid, Hf,V;2) = −2806.1307

L(bcc_A2, Hf,V;0) = 15,734.0738 + 7.5696*T

L(bcc_A2, Hf,V;1) = −5012.0000 − 5.1387*T

L(bcc_A2, Hf,V;2) = 2010.5626

L(cph_A3, Hf,V;0) = 33,560.0000 + 1.9000*T

G(C15-LAVES,Hf:V;0) − 0.33333*H298(CPH_A3,Hf;0) − 0.66667* H298(BCC_A2,V;0) = −12,330.1803 + 0.8168*T + 0.33333*GHFBCC + 0.66667*GVFCC

I-2-2. Modeling of the C15-Laves Phase with a Composition Range: $(Hf,V)_{0.33333}(Hf,V)_{0.66667}$

L(liquid, Hf,V;0) = −18,769.2667 + 11.2873*T

L(liquid, Hf,V;1) = −13,370.3477 + 2.0192*T

L(liquid, Hf,V;2) = −2879.9773

L(bcc_A2, Hf,V;0) = 16,044.6921 + 7.4180*T

L(bcc_A2, Hf,V;1) = −5012.0000 − 5.1387*T

L(bcc_A2, Hf,V;2) = 2010.5626

L(cph_A3, Hf,V;0) = 33,560.0000 + 1.9000*T

G(C15-LAVES,Hf:Hf;0) − H298(CPH_A3,Hf;0) = +5000 + GHFBCC

G(C15-LAVES,V:V;0) − H298(BCC_A2,V;0) = +5000 + GVFCC

$$G(C15\text{-LAVES,Hf:V;0}) - 0.33333*H298(\text{CPH\_}A3\text{,Hf;0}) - 0.66667*H298(\text{BCC\_}A2\text{,V;0}) = -11{,}938.6881 + 0.8507*T + 0.33333*\text{GHFBCC} + 0.66667*\text{GVFCC}$$

$$G(C15\text{-LAVES,V:Hf;0}) - 0.33333*H298(\text{BCC\_}A2\text{,V;0}) - 0.66667*H298(\text{CPH\_}A3\text{,Hf;0}) = 11{,}938.688 - 0.8507*T + 0.33333*\text{GVFCC} = + 0.66667*\text{GHFBCC} + 10{,}000$$

$$L(C15\text{-LAVES,Hf:Hf,V;0}) = 22{,}166.9330$$

II. V-Zr System

II-1. C15-Laves Phase with Reference States bcc_A2 V and cph_A3 Zr

II-1-1. Modeling of the C15-Laves Phase as Stoichiometric: $Zr_{0.33333}V_{0.66667}$

$$L(\text{liquid,V,Zr;0}) = -17{,}401.8117 + 14.2689*T$$

$$L(\text{liquid,V,Zr;1}) = -868.4157 + 3.1097*T$$

$$L(\text{liquid,V,Zr ;2}) = 3201.7954$$

$$L(\text{bcc\_}A2\text{,V,Zr;0}) = 1906.0284 + 19.4653*T$$

$$L(\text{bcc\_}A2\text{,V,Zr;1}) = -6506.2003 + 8.8643*T$$

$$L(\text{bcc\_}A2\text{,V,Zr;2}) = -2623.0285$$

$$L(\text{cph\_}A3\text{,V,Zr ;0}) = 15{,}000 + 0.1*T$$

$$G(C15\text{-LAVES,Zr:V;0}) - 0.33333*H298(\text{CPH\_}A3\text{,Zr;0}) - 0.66667*H298(\text{BCC\_}A2\text{,V;0}) = -5000.0000 + 1.8000*T + 0.33333*\text{GHSERZR} + 0.66667*\text{GHSERVV}$$

II-1-2. Modeling of the C15 Laves Phase with a Composition Range: $(V,Zr)_{0.33333}\ (V,Zr)_{0.66667}$

$$L(\text{liquid,V,Zr;0}) = -17{,}401.8117 + 14.2689*T$$

$$L(\text{liquid,V,Zr;1}) = -868.4156 + 3.1097*T$$

$$L(\text{liquid,V,Zr;2}) = 3201.7954$$

$$L(\text{bcc\_}A2\text{,V,Zr;0}) = 2253.9668 + 19.4731*T$$

$$L(\text{bcc\_}A2\text{,V,Zr;1}) = -9657.3231 + 10.8995*T$$

$$L(\text{bcc\_}A2\text{,V,Zr;2}) = -593.4275$$

$$L(\text{cph\_}A3\text{,V,Zr;0}) = 18{,}619.6518 + 2.0608*T$$

$$G(C15\text{-LAVES,Zr:Zr;0}) - H298(\text{CPH\_}A3\text{,Hf;0}) = +5000 + \text{GHSERZR}$$

$$G(C15\text{-LAVES,V:V;0}) - H298(\text{BCC\_}A2\text{,V;0}) = +5000 + \text{GHSERVV}$$

$$G(C15\text{-LAVES,Zr:V;0}) - 0.33333*H298(\text{CPH\_}A3\text{,Zr;0}) - 0.66667*H298(\text{BCC\_}A2\text{,V;0}) = -4785.7904 + 1.9173*T + 0.33333*\text{GHSERZR} + 0.66667*\text{GHSERVV}$$

$$G(C15\text{-LAVES,V:Zr;0}) - 0.33333*H298(\text{BCC\_}A2\text{,V;0}) - 0.66667*H298(\text{CPH\_}A3\text{,Zr;0}) = 4785.7904 - 1.9173*T + 0.33333*\text{GHSERVV} + 0.66667*\text{GHSERZR} + 10{,}000$$

$$L(C15\text{-LAVES,V,Zr:V;0}) = 94{,}451.2785$$

$$L(C15\text{-LAVES,V:V,Zr;0}) = 7067.4166$$

$$L(C15\text{LAVES,V,Zr:Zr;0}) = 18{,}439.6970 + 0.7532*T$$

II-2. C15-Laves Phase with Reference States fcc_A1 V and bcc_A2 Zr

II-2-1. Modeling of the C15-Laves Phase as Stoichiometric: $Zr_{0.33333}V_{0.66667}$

$$L(\text{liquid,V,Zr;0}) = -16{,}815.1576 + 13.0144*T$$

$$L(\text{liquid,V,Zr;1}) = -1188.0661 + 3.3048*T$$

$$L(\text{liquid,V,Zr;2}) = 3327.3775$$

$$L(\text{bcc\_}A2\text{,V,Zr;0}) = 1986.3760 + 19.1190*T$$

$$L(\text{bcc\_}A2\text{,V,Zr;1}) = -7650.8542 + 9.6845*T$$

$$L(\text{bcc\_}A2\text{,V,Zr;2}) = -2357.0407$$

$$L(\text{cph\_}A3\text{,V,Zr;0}) = 17{,}400.0000 + 0.1000*T$$

$$G(C15\text{-LAVES,Zr:V;0}) - 0.33333 \times H298(\text{CPH\_A3,Zr;0}) - 0.66667 \times H298(\text{BCC\_}A2\text{,V;0}) = -12{,}118.0385 + 1.9240 \times T + 0.33333 \times \text{GZRBCC} + 0.66667 \times \text{GVFCC}$$

II-2-2. Modeling of the C15 Laves Phase with a Composition Range: $(V,Zr)_{0.33333}\ (V,Zr)_{0.66667}$

$$L(\text{liquid,V,Zr;0}) = -15{,}681.2606 + 12.3118 \times T$$

$$L(\text{liquid,V,Zr;1}) = -1031.4917 + 3.2131 \times T$$

$$L(\text{liquid,V,Zr;2}) = 3511.6675$$

$$L(\text{bcc\_}A2\text{,V,Zr;0}) = 1662.8111 + 19.2919 \times T$$

$$L(\text{bcc\_}A2\text{,V,Zr;1}) = -9617.8130 + 10.9230 \times T$$

$$L(\text{bcc\_}A2\text{,V,Zr;2}) = -1871.4524$$

$$L(\text{cph\_}A3\text{,V,Zr;0}) = 17{,}600.3217 + 1.2714 \times T$$

$$G(C15\text{-LAVES,Zr:Zr;0}) - H298(\text{CPH\_}A3\text{,Hf;0}) = +5000 + \text{GZRBCC}$$

$$G(C15\text{-LAVES,V:V;0}) - H298(\text{BCC\_}A2\text{,V;0}) = +5000 + \text{GVFCC}$$

$$G(C15\text{-LAVES,Zr:V;0}) - 0.33333 \times H298(\text{CPH\_}A3\text{,Zr;0}) - 0.66667 \times H298(\text{BCC\_}A2\text{,V;0}) = -12{,}617.8161 + 2.5115 \times T + 0.33333 \times \text{GZRBCC} + 0.66667 \times \text{GVFCC}$$

$$G(C15\text{-LAVES,V:Zr;0}) - 0.33333 \times H298(\text{BCC\_}A2\text{,V;0}) - 0.66667 \times H298(\text{CPH\_}A3\text{,Zr;0}) = +12{,}617.8181 - 2.5115 \times T + 0.33333 \times \text{GVFCC} + 0.66667 \times \text{GZRBCC} + 10{,}000$$

$$L(C15\text{-LAVES,V,Zr:V;0}) = 858.6956$$

$$L(C15\text{-LAVES,V,Zr:Zr;0}) = 22{,}937.6788$$

References

1. R. Kieffer, H. Nowotny, P. Ettmayer, and L. User, Zur entmischung von kubischen merhrstoffcarbiden, *Monatsh. Chem.,* Vol 99, 1968, p 1020
2. R. Kieffer, Preparation and Properties of Interstitial Compounds, *J. Inst. Met.,* Vol 97, 1969, p 164-172
3. S. Hamar-Thibault, L. Adnane, and R. Kesri, Miscibility of Binary VC–MC Carbides in Quaternary Fe–V–M–C Alloys, *J. Alloy. Compd.,* Vol 317-318, 2001, p 311-314
4. P. Fernandez, A.M. Lancha, J. Lapenna, and M. Hernandez-Mayoral, Metallurgical Characterization of the Reduced Activation Ferritic/Martensitic Steel Eurofer'97 on As-received Condition, *Fusion Eng. Des.,* Vol 58-59, 2001, p 787-792
5. M. Grujicic, I.J. Wang, and S. Owen, On the Formation of Duplex Precipitate Phases in an Ultra-Low Carbon Microalloyed Steel, *Calphad,* Vol 12, 1988, p 261-275
6. C.A. Danon and C. Servant, A Thermodynamic Evaluation of the Ta-V System, *J. Alloy. Compd.,* Vol 366, 2004, p 191-200
7. A. Fernandez Guillermet, Analysis of Thermodynamical Properties and Phase Stability in the Zirconium-Carbon Systems, *J. Alloy. Compd.,* Vol 217, 1995, p 69-89
8. A. Fernandez Guillermet, Thermodynamic Analysis of Stable Phases in the Zr-Nb System and Calculation of the Phase Diagrams, *Z. Metallkde.,* Vol 82, 1991, p 478-487
9. A. Fernandez Guillermet, Phase Diagram and Thermochemical Properties of the Zr-Ta System. An Assessment Based on Gibbs Energy Modelling, *J. Alloy. Compd.,* Vol 226, 1995, p 174-184
10. J. Korb and K. Hack, GTT, System V-Zr, Germany, 1995, in Cost 507, Definition of Thermochemical and Thermophysical Properties to Provide a Database for the Development of New Light Alloys, *Thermodynamical Database for Light Metal Alloys,* I. Ansara, A.T. Dinsdale, and M.H. Rand, Ed., Vol 2, 1998, p 303-304
11. L. Kaufman and H. Bernstein, *Computer Calculation of Phase Diagrams,* Academic Press, 1970
12. H. Sawa and S. Wakao, Electrochemical Properties of Zr-V-Ni System Hydrogen-Absorbing Alloys of Face Centered Cubic Structure, *Mater. Trans., JIM,* Vol 31, 1990, p 487-492
13. W. Daumer, H.R. Khan, Y. Kobber, and K. Luders, Temperature Dependent Magnetic Susceptibility and Superconductivity of Cubic Laves Phase (C15) Hydrides: $V_2Hf_{0.5}Zr_{0.5}Hx$ (0x 4.8), *Phys. Lett. A,* Vol 138, 1989, p 323-328
14. W.Y. Kim, D.E. Luzzi, and D.P. Pope, Room Temperature Deformation Behavior of the Hf-V-Ta C15 Laves Phase, *Intermetallics,* Vol 11, 2003, p 257
15. P. File, *Binaries Edition Inorganic Materials Database and Design System,* P. Villars, JTS, Tokyo, Japan and MPDS, Vitznau, Switzerland, version 1.0, 2002
16. E. Rudy and S. Windisch, The Phase Diagrams Hafnium-Vanadium and Hafnium-Chromium, *J. Less-Common Met.,* Vol 15, 1968, p 13-27
17. J.F. Smith, Hf-V (Hafnium-Vanadium), *Binary Alloy Phase Diagrams,* Vol 3, 2nd ed., T.B. Massalski, Ed., ASM International, 1990, p 2121-2124
18. S. Komjathy, The Constitution of Some Vanadium Base Binary and Ternary Systems and the Ageing Characteristics of Selected Ternary Alloys, *J. Less-Common Met.,* Vol 3, 1961, p 468-488
19. L.S. Guzei, E.M. Sokolovskaya, I.G. Sokoleva, E.I. Belyaeva, G.N. Romani, and S.N. Kuznetsov, Phase Diagram of the Vanadium-Hafnium System, *Moscow Univ. Chemi. Bull.,* Vol 23 (No. 4), 1968, p 35-37
20. G. W. Cunnigham, Nuclear Poisons, *React. Mater.,* Vol 6, 1963, p 63-66
21. J.F. Smith, V-Zr (Vanadium-Zirconium), *Binary Alloy Phase Diagrams,* 2nd ed., T.B. Massalski, Ed., ASM International, Vol 3, 1990, p 3528-3531
22. J.T. Williams, Vanadium-Zirconium Alloy System, *Trans. AIME,* Vol 203, 1955, p 345-350
23. W. Rostoker and A. Yamamoto, A Survey of Vanadium Binary Systems, *Trans ASM,* Vol 46, 1954, p 1136-1167
24. L.A. Petrova, On the Stabilization of the β-Solid Solution in Zirconium Alloys, *Izv. Akad. Nauk SSSR, Otd. Tekh. Nauk Metall. Topl.,* Vol 6, 1962, p 159-161
25. F.R. de Boer, R. Boom, W.C.M. Mattens, A.R. Miedema, and A.K. Niessen, *Cohesion in Metals: Transition Metal Alloys,* F.R. de Boer and D.G. Pettifor, Ed., North-Holland, 1988
26. A.R. Miedema, P.F. de Châtel and F.R. de Boer, Cohesion in Alloys—Fundamentals of a Semi-Empirical Model, *Phys. B,* Vol 100, 1980, p 1-28
27. P. Villars and L.D. Calvet, *Pearson's Handbook of Crystallographic Data for Intermetallic Phases,* 2nd ed., American Society for Metals, 1986
28. N. Dupin and I. Ansara, Thermodynamic Assessment of the Cr-Ta System, *J. Phase Equilibria,* Vol 14, 1993, p 451-456
29. N. Dupin and I. Ansara, Thermodynamic Assessment of the Cr-Ni-Ta System, *Z. Metallkde.,* Vol 81, 1990, p 49
30. C. Wagner and W. Schottky, Theorie der geordneten Mischphasen, *Z. Phys. Chem.,* Vol 11, 1930, p 163
31. A.T. Dinsdale, SGTE Data for Pure Elements, *Calphad,* Vol 15 (No. 4), 1991, p 317-425
32. O. Redlich and A. Kister, *Ind. Eng. Chem.,* Vol 40, 1948, p 345-348
33. H.K. Hardy, A "Sub-Regular" Solution Model and Its Application to Some Binary Alloy Systems, *Acta Metall.,* Vol 1, 1953, p 202-209
34. B. Sundman, B. Jansson, and J.-O. Andersson, The Thermo-Calc Databank System, *Calphad,* Vol 2 (No. 9), 1985, p 153-190
35. F. Zhang, S.-L. Chen, Y.A. Chang, and W.A. Oates, An Approach for Obtaining Thermodynamic Descriptions of Intermetallic Phases: Application to the Cr-Ta System, *Intermetallics,* Vol 9, 2001, p 1079-1083
36. C. Servant and A. Danon, CALPHAD Modelling of the Unmixing of Transition Metal Carbide Phases, *Calphad,* December 2004, in press
37. A.A. Rempel, A.I. Gusev, and G.P. Shveikin, Thermodynamic Calculation of the Phase Diagrams of the $VC_{0.88}$-NbC, $VC_{0.88}$-TaC, $VC_{0.88}$-HfC, NbC-TaC, and NbC-HfC Systems, *Russ. J. Phys. Chem.,* Vol 58 (No. 9), 1984, p 1322-1325